UNIVERSITÀ DI SIENA 1240

Dipartimento di Medicina Molecolare e dello Sviluppo

Dottorato in Medicina Molecolare

XXXV° Ciclo

Coordinatore: Prof.Vincenzo Sorrentino

Characterization of the effect of Calsequestrin 1 mutations identified in tubular aggregate myopathies on calcium homeostasis in mouse FDB fibers

Settore scientifico disciplinare: MED/04

Candidato/a

Dr. Claudio Nanni

Università degli Studi di Siena

Firma digitale del/della candidato/a

Claudio Nanni

Firmato da
CLAUDIO NANNI
Data: 25/04/2023
09:56:38 CEST

Supervisore

Prof.ssa Alessandra Gamberucci

Università degli Studi di Siena

Co-supervisore

Prof. Vincenzo Sorrentino

Università degli Studi di Siena

Anno accademico di conseguimento del titolo di Dottore di ricerca

2022/23

Università degli Studi di Siena
Dottorato in Medicina Molecolare
XXXV° Ciclo

Data dell'esame finale

_____

Commissione giudicatrice

_____
_____
_____
_____
_____

Supplenti

_____
_____

Contents

1. INTRODUCTION 1
1.1-MUSCLE FIBERS 2
1.2-CALCIUM HOMEOSTASIS 8
1.3-CALSEQUESTRIN 12
1.4-STORE-OPERATED CALCIUM ENTRY 16
1.5-TUBULAR AGGREGATE MYOPATHY 21
2.AIM OF THE STUDY 25
3- MATERIALS AND METHODS 27
3.1- ANIMALS 28
3.2- PLASMID PREPARATION 28
3.3 FDB MUSCLE TRANSFECTION 30
3.4 FDB FIBERS ISOLATION 31
3.5 MEASUREMENT OF CALCIUM RETICULAR STORES 32
3.6 CALCIUM INFLUX MEASUREMENT 33
3.7 NORMALIZATION AND STATISTICS 34
4.RESULTS 36
4.1 TRANSFECTED CASQ1 IS CORRECTLY EXPRESSED IN FDB FIBERS 37
4.2 TRANSFECTION CAN RESTORE CALCIUM BUFFERING ABILITY IN KO FIBERS 38
4.3 RETICULAR CALCIUM CONTENT IS REDUCED IN CASQ1 MUTANTS 39
4.4 MUTATIONS SUPPRESS CASQ1 INHIBITION OF SOCE 42
5. DISCUSSION 45
6. BIBLIOGRAPHY 51

1. INTRODUCTION

1.1-MUSCLE FIBERS

Muscle tissue is one of the four basic types of tissue in our body.

It is responsible for voluntary and involuntary movements of the body and can be divided into smooth, striated, and cardiac tissue.

Striated muscle is composed of two major muscle types, skeletal and cardiac.

Skeletal muscle, which compose about 35% of the weight of a human body have a plethora of functions including producing movement, maintaining body posture, controlling body temperature, and stabilizing joints.

Skeletal muscles are substantially composed of multinucleated contractile muscle fibres called myocytes. A single muscle fibre can contain from hundreds to thousands of nuclei. Each myofiber contain several myofibrils. Bundles of myofibers form the fascicles, and bundles of fascicles form the muscle tissue.

The basic cellular unit within a muscle fibre is called the sarcomere, and its complex architecture is what allows the muscles to work.

Sarcomeres represent a complex structure composed of two main alternating sets of protein filaments: thin filaments and thick filaments.

Visually, the sarcomere is bordered at each end by a dark narrow line called the Z-disk. Each Z-disk bisects a lighter I band. At the centre of the sarcomere is a dense A-band made up of thick filaments, with a lighter H-zone. The M-line bisects the H-band. Thin filaments are held together, in a lateral array, at the Z-disk while the M-line interconnects the thick filaments.

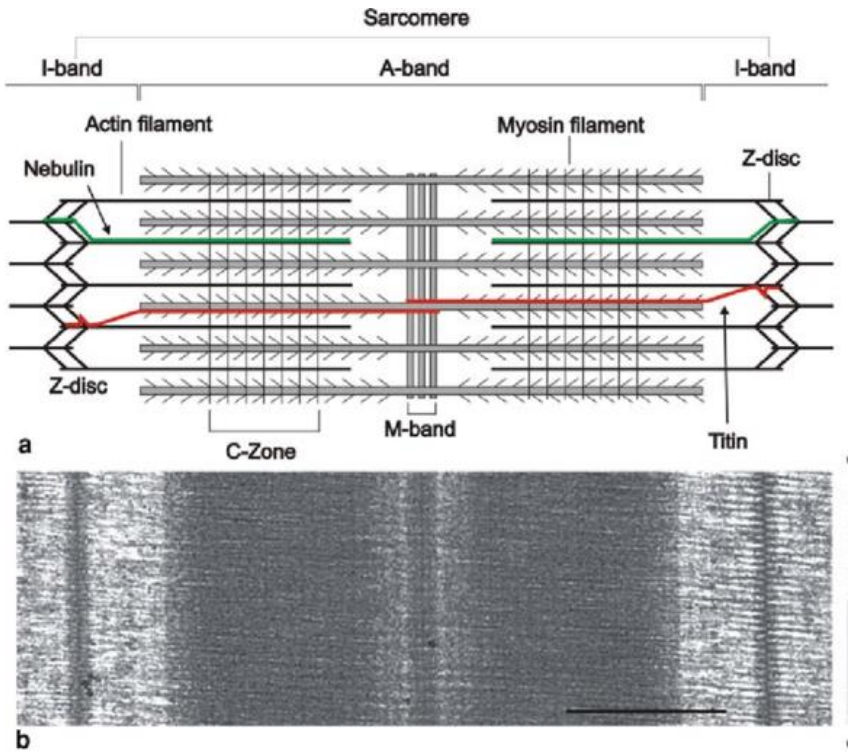

Figure 1: Striated muscle sarcomere. A) Schematic diagram showing the main components of the sarcomere. The A-band comprises myosin filaments crosslinked at the centre by the M-band assembly. Thin actin-containing filaments are tethered at their barbed end at the Z-disc and interdigitate with the thick filaments in the A-band. B) Electron micrograph of a longitudinal section of fish white (fast) muscle showing details of the sarcomere (Luther, Pradeep; 2009).

Thick filaments are mainly composed by myosin protein.

Myosin contains two heavy chains, which constitute the head and tail domains. Each of these heavy chains contains the N-terminal head "motor" domain, which bears ATPase activity and binds actin in the thin filaments, while the C-terminal tails take on a coiled-coil morphology, holding the two heavy chains together.

It also contains four light chains, two essential light chains, and two regulatory light chains, resulting in two per head. These bind the heavy chains in the "neck" region between the head and tail. In addition to myosin, a number of other proteins reside in the thick filament playing important structural and regulatory roles. These include myosin binding protein-C (MyBP-C), titin, myomesin, and obscurin. MyBP-C is tightly anchored to the thick filament through binding to both myosin and titin and

modulates the formation and cycling of actomyosin cross-bridges. Titin, the largest known protein to date, is intimately bound to myosin along the length of the thick filament, and mainly functions as a scaffold for thick filament assembly. Myomesin forms antiparallel homodimers cross-linking myosin molecules within the M-band and contributing to the elasticity of the thick filament. Lastly, obscurin, the newest giant protein of muscle cells, contributes to the stabilization of thick filaments into mature A-bands and their alignment with internal membrane systems (Wang L & Geist J, 2018).

Thin myofilaments consist of an axis taking the shape of a double helix formed by the reciprocal coiling of two filaments of F-actin, a polymeric protein consisting of globular subunits of G-actin.

Thin filaments are associated with some proteins that facilitate contraction.

Most important of them are troponin and tropomyosin.

Troponin itself has three subunits: Tn-I, the inhibitory subunit that binds to actin; Tn-C, the Ca^{2+} binding subunit and Tn-T, the tropomyosin binding component.

Tropomyosin, instead, stabilizes the binding of actin to myosin. (Mukund & Subramaniam, 2020).

During contraction the thin filaments slide along the thick filaments toward the centre of the sarcomere. As a result, the H band and I hemi bands shorten, as does the entire sarcomere, whereas the length of the A band does not change with contraction.

Surrounding the myofibrils of striated muscle cells, there is a system of tubules which is called sarcoplasmic reticulum (SR), a specialized version of the smooth endoplasmic reticulum of other eukaryotic cells. The sarcoplasmic reticulum contains several proteins, some of which support Ca^{2+} storage and release, while others regulate the

formation and maintenance of this highly convoluted organelle and mediate the interaction with other components of the muscle fibre.

The SR can be divided into two domains, the longitudinal SR and the junctional SR.

The longitudinal SR is composed of numerous tubules interconnected with each other forming a network around each myofibril. At their ends, the longitudinal tubules melt into a single dilated sac called terminal cisterna. Two terminal cisternae and one T-tubule form a triad. T-tubules are invaginations of the plasma membrane that transversely extend into muscle fibres. (Rossi et al., 2022)

The main function of the sarcoplasmic reticulum is to regulate the Ca^{2+} homeostasis, with the longitudinal SR representing the sites of Ca^{2+} uptake and storage and the junctional SR representing the sites of Ca^{2+} release.

The triad, consisting of terminal cisternae and T-tubules, represents the membrane platform where several dedicated proteins operate in transducing the depolarization of the plasma membrane into Ca^{2+} release from the SR, a mechanism known as excitation–contraction coupling (ECC).

The ECC phenomenon represents a fast communication between electrical events occurring in the plasma membrane and Ca^{2+} release from the SR, which leads to muscle contraction. (Calderón, Bolaños and Caputo, 2014)

Activation begins when an action potential from a motor neuron arrives at the neuromuscular junction and causes the neurotransmitter acetylcholine to be released into the postsynaptic cleft.

The opening of acetylcholine receptors produces a local depolarization, called the end-plate potential, which brings the postsynaptic membrane to threshold potential for exciting an action potential.

An action potential is then generated, as a result of which depolarization occurs along the sarcolemma (the plasma membrane of striated muscle cells): this occurs thanks to voltage-dependent sodium channels on the sarcolemma.

The propagation of the potential continues along the sarcolemma through the T tubules, where the dihydropyridine-sensitive receptor (DHPR) is located.

The dihydropyridine-sensitive receptor (DHPR) is an L-type Ca^{2+} channel, which, with the change of action potential, changes its conformation and is activated, allowing the entry of Ca^{2+} ion.

This conformational change is also transmitted into the sarcoplasmic reticulum region, where the ryanodine-sensitive receptor (RyR1) is located: it opens allowing Ca^{2+} to escape from the sarcoplasmic reticulum into the sarcoplasm (the cytoplasm of the striated muscle cells).

At this stage, the free Ca^{2+} in the cytoplasm goes to bind to the C subunit of troponin (Tn-C) inducing a conformational change that drags the T subunit (Tn-T), which was bound to tropomyosin.

Subsequently on the actin binding site, previously occupied by tropomyosin, will be bound myosin, leading to the phenomenon of muscle contraction. This occurs by exploiting the energy obtained from the hydrolysis of ATP, carried out by the ATPase domain of the head of myosin.

When the propagation of the potential comes to an end, the C subunit of troponin dissociates from Ca^{2+}, which is brought back into the sarcoplasmic reticulum thanks to an ATPase pump, called SERCA (SERCA: Sarcoplasmic Endoplasmic Reticulum Calcium ATPase), that will be described more extensively in the next chapter.

It is the gradual decrease of Ca^{2+} in the cytoplasm that causes the end of the contraction mechanism.

1.2-CALCIUM HOMEOSTASIS

Calcium ions play a vital role in the physiology and biochemistry of the body.

They play an important role in signal transduction pathways, where they act as a second messenger, but also in the release of neurotransmitters from neurons, in the contraction of all types of muscle cells, and in fertilization.

Ca^{2+} concentration is very high in the extracellular environment and organelles (especially in the endoplasmic reticulum), while it is extremely low in the cytosol.

Although SERCAs represent the key enzymes that contribute to sarcoplasmic Ca^{2+} clearance following muscle contraction, a trans-sarcolemma flux toward the extracellular environment also occurs in striated muscles. This is mediated by Plasma Membrane Calcium ATPases (PMCAs) and Na^{+}/Ca^{2+} exchangers localized in the sarcolemma.

PMCA belongs to the P-type transport ATPase family.

These pumps are high affinity Ca^{2+} extruders, binding a single intracellular Ca^{2+} ion which is then deposited to the extracellular space following conformational changes which first allow transport of the ion through the plasma membrane and finally dissociation from the pump through lowering its Ca^{2+} affinity. (Rossi et al. , 2022)

The general structure of the PMCA, like other members of the P-type ATPase family, consists of 10 hydrophobic trans-membrane domains flanked by cytosolic NH_2 and COOH terminals, and with two large intracellular loops. (Stafford *et al.*, 2017)

Located on the sarcoplasmic reticulum, there is one other protein involved in the maintenance of Ca^{2+} homeostasis, named SERCA (Sarco-Endoplasmic Reticulum Calcium ATPase).

SERCA is an ~110-kDa transmembrane protein that belongs to the family of P-type ion-translocating ATPases and plays a critical role in the control of cytosolic Ca^{2+} concentration, it can transport two Ca^{2+} ions for each hydrolysed ATP.

In vertebrates, SERCA pumps are encoded by three different genes, named ATP2A1-3. More than 10 protein variants are generated through alternative splicing occurring in the 3'-end of the main transcripts The SERCA2a isoform is expressed in both cardiac and slow-twitch skeletal muscles, whereas the fast-twitch skeletal muscle expresses SERCA1a and SERCA1b.

The SERCA pump is made up of a single polypeptide chain folded into four major domains: a transmembrane region consisting of 10 helical segments (TM1 to TM10, which include two Ca^{2+}-binding sites), and three cytosolic domains named A (actuator), N (nucleotide-binding), and P (phosphorylation). (Avila *et al.*, 2019)

An essential role in the activation of muscle contraction is played by the cooperation of the dihydropyridine-sensitive receptor (DHPR) with the ryanodine-sensitive receptor (RyR1).

DHPR is a voltage-gated Ca^{2+} channel belonging to the voltage-dependent superfamily of Ca^{2+} channel. It is an heteromultimeric complex consisting of $\alpha 1_s$ (212 kDa), $\alpha 2\text{-}\delta_1$ (125 kDa), $\beta 1_a$ and γ_1 subunits.

The $\alpha 1_s$ subunit contains the major functional domains of the channel. It is an integral membrane protein that contains the pore-forming and voltage-sensing regions, as well as the binding site for dihydropyridines.

DHPR is capable of functioning both as a voltage sensor for EC coupling and as a Ca^{2+} ion channel. (Jerry P. Eu & Gerhard Meissner, 2012)

The release of Ca^{2+} ions from the sarcoplasmic reticulum is a key step in a wide variety of biological functions. The sarcoplasmic reticulum Ca^{2+}-release channels are commonly referred to as ryanodine receptors (RyRs).

RyRs are a family of Ca^{2+} release channels that represent the largest ion channels known to date, there are three RyR isoforms: RyR1 is the main isoform in skeletal muscle, RyR2 can be found in cardiac muscle and RyR3 is expressed in many tissues, including diaphragm, smooth muscle and brain. (Jerry P. Eu & Gerhard Meissner, 2012)

RyRs are homotetramers with a total molecular weight greater than 2.2 MDa that consist of a transmembrane domain forming anion-conductive pore, regulated by a large N-terminal cytoplasmic domain. In the cytoplasmic region, many domains have been described, referred to as subregions, which represent binding sites for several auxiliary proteins and molecules that contribute to regulating the opening and closing of the channel.

The cytoplasmic domains of RyR1 interacts with Ca^{2+} and Mg^{2+} ions, but also with ligands such as ATP, caffeine and ryanodine, and accessory proteins such as calmodulin, even if Calmodulin (CaM) was proposed to bind at different regions of RyR1 channels, acting either as a weak activator, at nanomolar Ca^{2+} concentration, or, in the micromolar range, as a channel inhibitor. One of the proposed binding sites for CaM also binds the EF-hand protein S100, a protein also able to activate the channel.

Moreover, RyR1 interacts, indirectly, with the voltage-gated Ca^{2+} channel, also known as the dihydropyridine receptor (DHPR).

In the SR lumen, the major Ca^{2+}-buffering protein, calsequestrin (CASQ), interacts with RyR1 indirectly through the membrane-anchored proteins triadin and junctin. (Chen & Kudryashev, 2020).

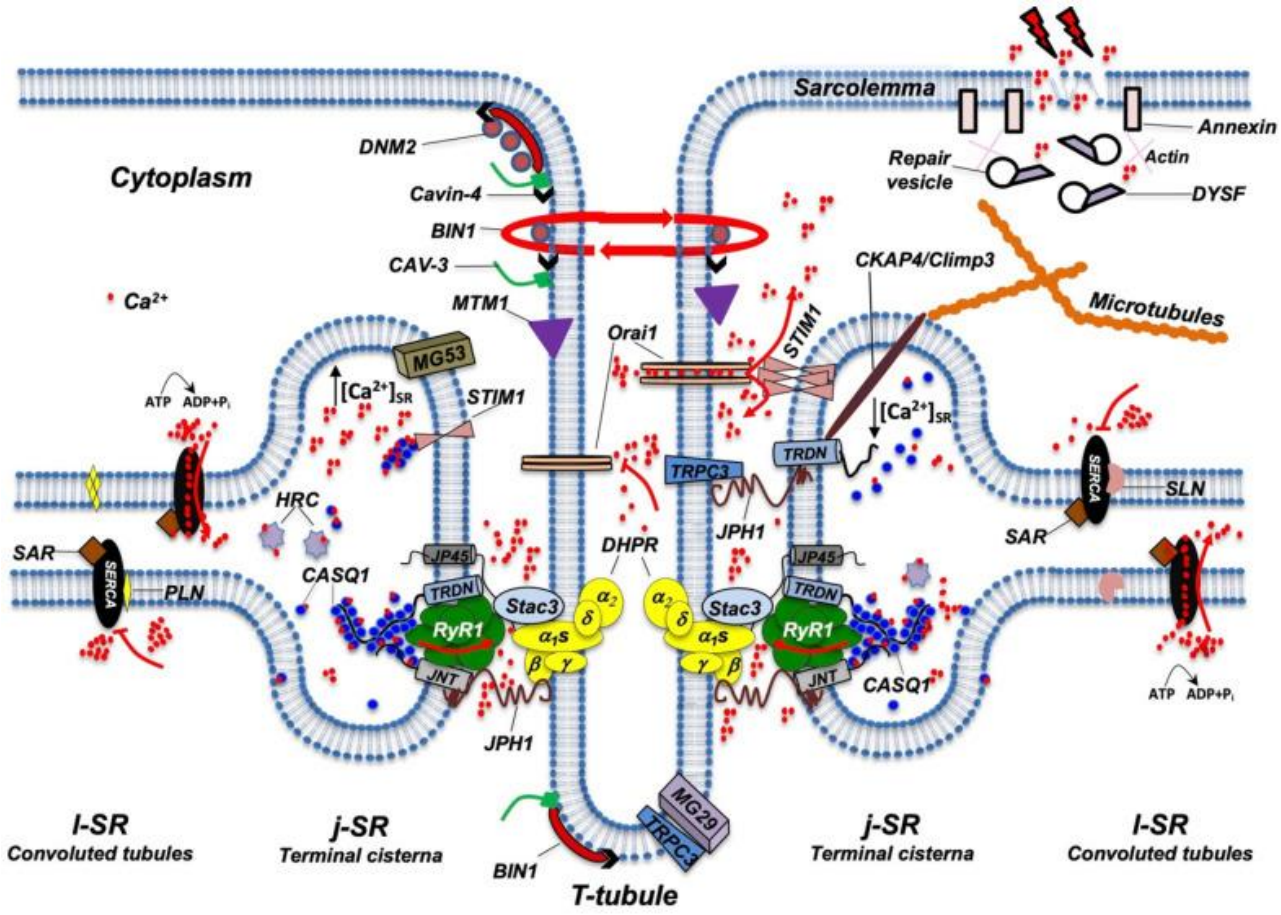

Figure 2: Schematic representation of the main proteins accommodated in TT, j-SR, and l-SR.

1.3-CALSEQUESTRIN

Calsequestrin (CASQ) is a protein of 45 kDa localized in the lumen of the sarcoplasmic reticulum of striated muscles where, thanks to its ability to bind Ca^{2+} with low affinity and high capacity, is responsible for Ca2+ storage in relationship with activation of muscle contraction.

Calsequestrin is an efficient Ca2+ storage protein and binds up to ~40 mol of Ca2+ per mol of protein with relatively low affinity. (Wang and Michalak, 2020)

In skeletal muscle, two isoforms of calsequestrin (CASQ) have been identified: CASQ1 and CASQ2. CASQ1 is expressed in fast- and slow-twitch skeletal muscle fibres, whereas CASQ2 is expressed in slow-twitch skeletal muscle fibres and in cardiac muscle The two isoforms present a high sequence homology and basically only differ in their acidic C-terminus. (Beard N.A., Laver D.R., Dulhunty A.F.,2004)

In the sarcoplasmic reticulum of skeletal muscle fibres, CASQ1 molecules exist as monomers when luminal Ca^{2+} concentration is lower than 10 μM. As luminal Ca^{2+} concentration increases, it undergoes molecule compaction, dimerization, and polymerization. (Wang et al., 2015)

Low concentrations of Ca^{2+} induce dimerization promoting front-to-front interactions between two adjacent monomers. With increasing levels of Ca^{2+}, polymer formation will take place, mediated by back-to-back interactions, which result in an increased ability to bind Ca^{2+}.

This finally results in the assembly of large ribbon-like structures, where negatively charged cavities may accommodate additional Ca^{2+}. CASQ1 polymerization is a

reversible process depending on the luminal Ca^{2+} concentration and the presence of CASQ-binding proteins or post-translational modification. (Kumar A., et al, 2013)

During sustained SR Ca^{2+} depletion, it was shown that almost all CASQ is present in its depolymerized status. In this condition, progressive closure of the RyRs was reported, with a consequent reduction in Ca^{2+} release aimed to prevent dangerous levels of SR Ca^{2+} depletion. Accordingly, it has been proposed that CASQ1 depolymerization may represent the intracellular switch that induces RyR1 closing. (Manno et al., 2017)

Essential, for calcium-induced polymerization to occur, is the acidic C-tail domain of calsequestrin: without this domain calsequestrin fails to polymerize in response to increased Ca^{2+} concentration. (Wang & Michalak, 2020)

CASQ1, along with other proteins, such as triadin, junctin and RyR1, are involved in the assembly of a quaternary complex implicated in the release of Ca^{2+} from the sarcoplasmic reticulum.

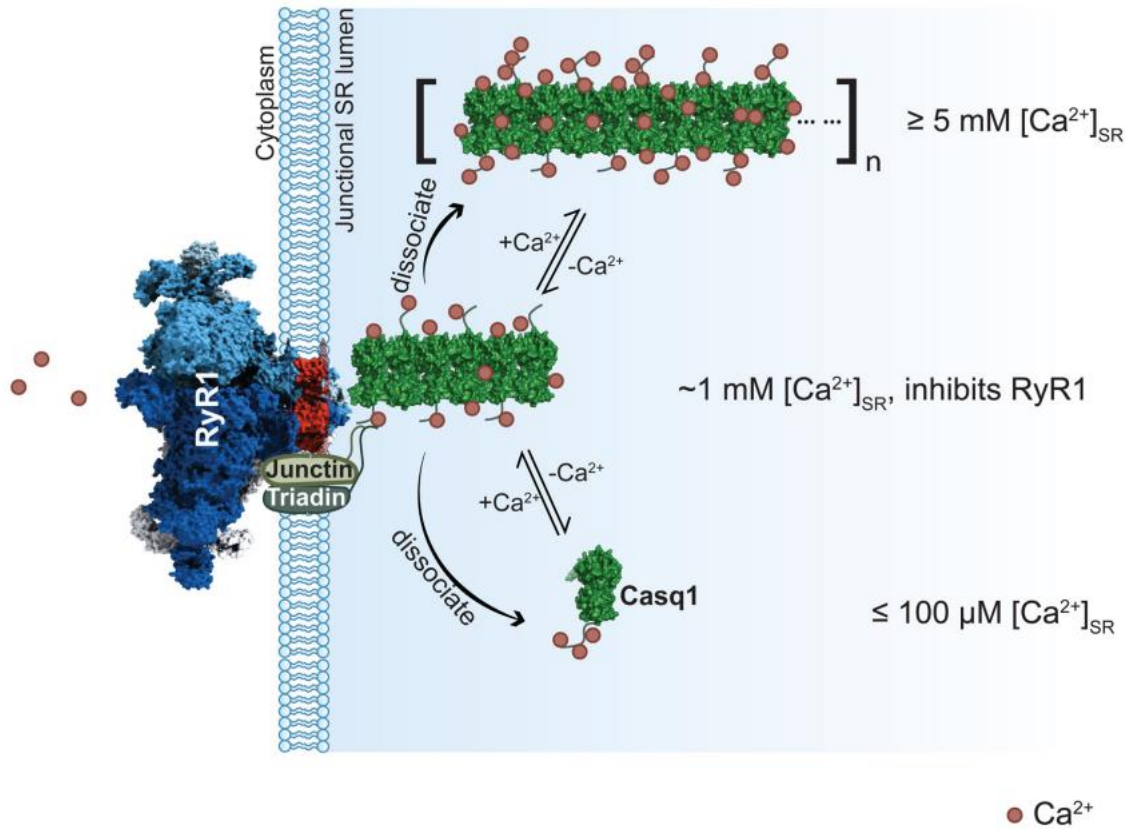

Fig.3: Relationship between calsequestrin and ryanodine receptor (RyR)/Ca^{2+} channel. SR, sarcoplasmic reticulum; RyR, ryanodine receptor/Ca^{2+} channel. (Wang, Q, Michalak,M, 2020)

CASQ1 mutations are associated with Tubular Aggregate Myopathy (TAM), while CASQ2 mutation are associated with CPVT, a form of cardiac arrhythmia.

Another function of this protein, aside from is Ca^{2+} buffering ability, is the regulation of SR ryanodine receptor (RyR).

In skeletal muscle, CASQ1 inhibits RyR1 at ≤1 mM [Ca^{2+}], but it dissociates from RyR1 at high Ca^{2+} concentration (≥5 mM). Removing CASQ1 from the RyR1 complex containing junctin, triadin, leads to increased duration of the opening of RyR1 channel.

The last important function associated with calsequestrin is related to store-operated Ca^{2+} entry (SOCE).

Store-operated Ca^{2+} entry functions are to replenish ER stores upon Ca^{2+} depletion.

In response to Ca^{2+} depletion, the ER luminal Ca^{2+} sensor, STIM1, dimerizes and interacts with the plasma membrane Ca^{2+} channel protein (ORAI1) to trigger Ca^{2+} entry from the extracellular space (Wang and Michalak, 2020).

The absence of calsequestrin in muscle tissue can lead to a variety of interesting structural changes. These changes can be seen as a combination of compensatory adaptations, developmental effects, and geometrical alterations. One of the most notable effects is a significant decrease in the size of the junctional sarcoplasmic reticulum cisternae. This decrease in volume is observed in both the extensor digitorum longus and soleus muscles but is particularly pronounced in the former where there is little calsequestrin present. This volume decrease is likely due to the lack of the luminal calsequestrin polymer that normally fills the junctional SR. This hypothesis is supported by other studies that have shown that calsequestrin-2 over-expression in murine myocardium induces the opposite effect, causing a drastic swelling of the SR terminal cisternae. These structural changes may have implications for muscle function and could potentially impact muscle performance. Further research is needed to fully understand the effects of calsequestrin ablation on muscle tissue structure and function (Paolini C, et al. 2007).

1.4-STORE-OPERATED CALCIUM ENTRY

Store-operated Ca^{2+} entry represents an important mechanism for the refilling of depleted intracellular reticulum Ca^{2+} stores.

SOCE is involved in a variety of important biological processes, including skeletal muscle contractility, smooth muscle migration and proliferation, breast cancer cell migration and metastasis, and endothelial proliferation. (Putney, 2011)

The SOCE pathway is operated by the coordinated activity of two main molecules: stromal interaction molecule 1 (STIM1) and calcium release-activated calcium channel protein 1 (Orai1). (Rossi et al., 2021)

There are two human STIM proteins, STIM1 and STIM2. Both are mostly located in the sarcoplasmic reticulum, though a minor amount of STIM1 is expressed at the cell surface.

STIM1 is a transmembrane protein (TM) of 685 amino acids incorporated into the ER/SR membrane. STIM1 possesses a signal peptide (Sig), a canonical EF hand domain (cEF) in the luminal ER portion, a hidden EF domain (hEF), an alpha sterile motif (SAM), a transmembrane domain (TM), three coiled-coil domains coil, CAD, a STIM1 domain ORAI1 activating region (SOAR), serine/proline rich domain (S/Proline), and lysine-rich domain (K-rich).

The established functions of STIM proteins are sensing Ca^{2+} in the SR lumen and communicating store depletion to other proteins, including ORAI1, in the plasma membrane.

On the other hand, regarding ORAI, there are three human ORAI proteins, ORAI1, ORAI2 and ORAI3. ORAI1 is a 33 kDa ubiquitous channel protein composed of 301

amino acids, both the NH_2 and COOH terminals reside in the cytoplasm, and each is implicated in the activation of ORAI1 through direct interactions with STIM1.

In unstimulated resting cells, STIM1 is diffusely distributed throughout the SR membrane, where it exists either as a monomer or as dimers.

After exposure of cells to stimuli that cause release of SR Ca^{2+}, the reduction in SR Ca^{2+} concentration leads to the dissociation of Ca^{2+} from the Ca^{2+}-binding helix-loop-helix structural domain (EF-hand motif) of STIM1, which consequently induces a conformational change and oligomerization of STIM1.

This is followed by a rapid translocation and accumulation of STIM1 in discrete multi-protein clusters or *punctae* in plasma membrane-associated ER (PAM) nanodomains, subcellular regions in which the PM and ER membranes are in close apposition and functionally interconnected.

Within PAM sites, STIM1 binds to and activates Orai1 Ca^{2+} channels via an interaction between a cytosolic motif of STIM1 known as the STIM1-ORAI activating region (SOAR) and a carboxy terminus α-helical region of Orai1. (Nelson et al., 2018) (**Fig.4**)

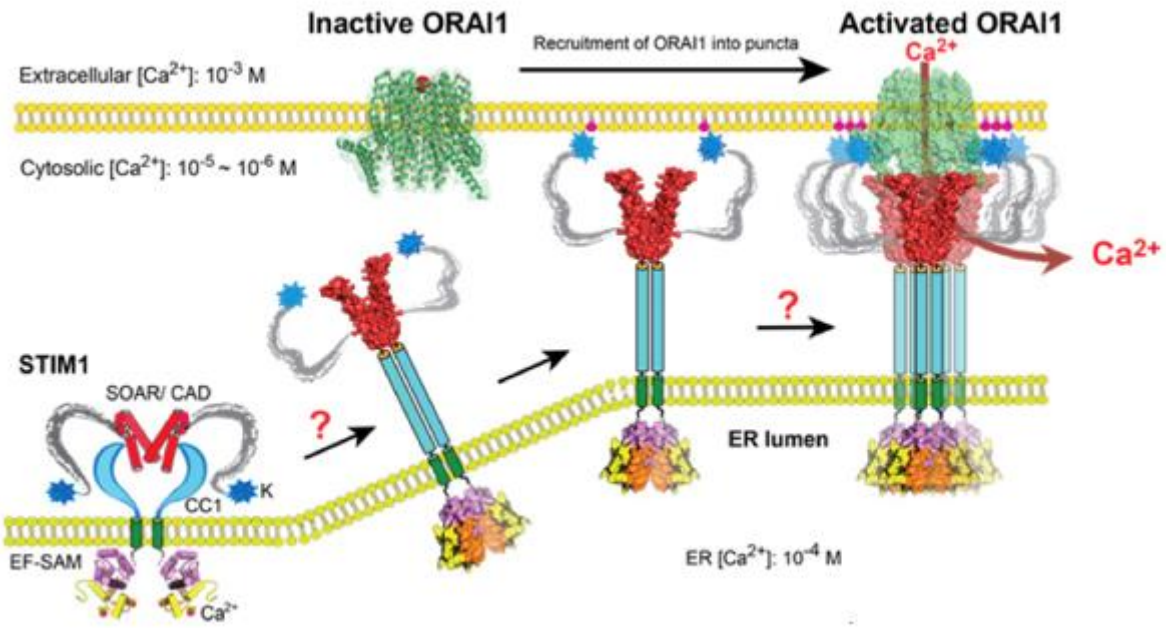

Figure 4: A tentative activation model of SOCE reflecting a STIM1 conformational switch and the dynamic coupling between STIM1 and ORAI1 (Ma, G.et al, 2015)

Given the crucial role that SOCE plays in the body, it has become essential to have available small molecules capable of modulating it, both positively and negatively.

Until 2018, the only known positive modulators of SOCE were boron-based compounds, such as 2-APB and MDEB.

Instead, in 2019, the first positive modulators that do not contain this element were reported, an example of which is 2T.

Among the negative modulators instead, in addition to lanthanides (La^{3+} and Gd^{3+}) several small molecules have been reported developed from a common progenitor called BTP2. (Serafini, Pirali, 2019)

Mutations in ORAI1 and STIM1 with pathological significance can be of two types: loss of function and gain of function.

The loss of function mutations is related to severe combined immunodeficiency (SCID), in which the patient is immunocompromised and subject to repeated infections, potentially lethal unless a transplant of stem cells is performed, but defects in SOCE proteins are also related to myopathy and increased muscle fatigability.
Gain of function mutations are responsible for a rare genetic disease, myopathy with tubular aggregates myopathies (TAM), which affects the muscle leading to muscle weakness, myalgia, cramps with very heterogeneous clinical outcomes that can lead up to heterogeneous outcomes that can lead to an impairment of the ability to movement.

In recent years, studies in SOCE postulated the existence of "calcium entry units" (CEUs): these are junctions within the I band of the sarcomere, between stacks of sarcoplasmic reticulum cisternae and the invaginations of t-tubule (Michelucci, et al. 2022). CEUs contains both STIM1 and Orai1 proteins, confirming their role in the spatial organization of SOCE. Has been proved that in wild-type mice exposed to acute exercise CEUs assemble, decaying several hours after, indicating a transient behaviour induced by exercise (Michelucci, A., 2018).
This CEUs seems to be constitutively assembled in CASQ1 KO mice, together with increased Orai1 expression, possibly indicating a compensatory constitutive activation of SOCE to provides a continuous flow of Ca^{2+} in absence of the buffering ability of CASQ1 (**Fig.5**).

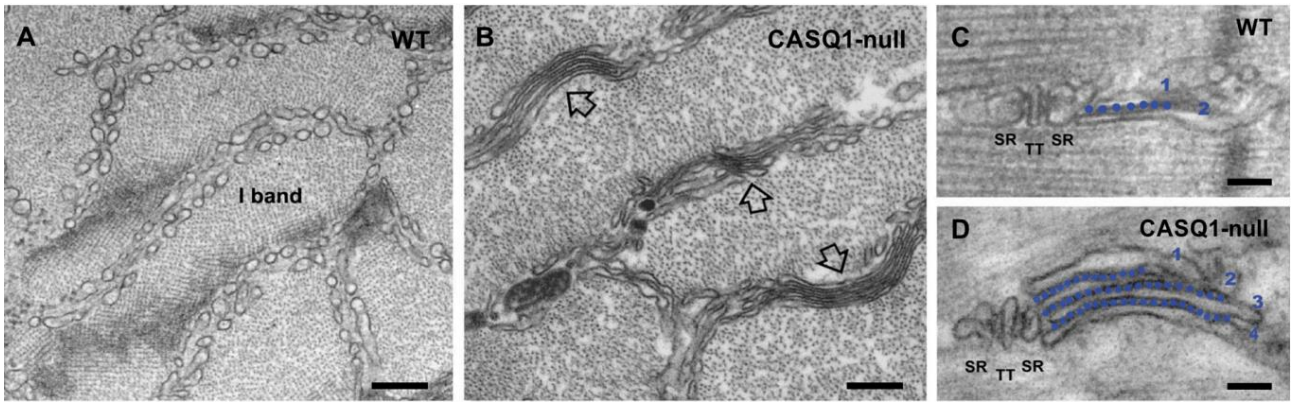

Figure 5: First report of CEUs. (**A and B**) Representative EM images of cross sections of EDL muscle fibres from WT (**A**) and CASQ1-null (**B**) mice (empty arrows point to stacks of SR membranes). (**C and D**) Representative EM images of longitudinal sections of EDL muscle fibres showing stacks of SR membranes in proximity to triads (SR-TT-SR). (Michelucci et al,2020)

1.5-TUBULAR AGGREGATE MYOPATHY

Tubular aggregate myopathy is a progressive muscle disease characterized by muscle weakness, cramping and myalgia. Some patients present additional clinical signs such as: miosis, thrombocytopenia, hyposplenism, ichthyosis, dyslexia, and short stature; this multi-systemic phenotype is called Stormorken syndrome (STRMK).

Most patients also display serum creatine kinase (CK) levels about 10-fold the normal upper limit, and some develop eye movement defects or contractures in the arms and legs. (Böhm and Laporte, 2018)

In muscle biopsies from patients with tubular aggregate myopathy, there are a set of tubular aggregates arising from clusters of sarcoplasmic reticulum membranes. In particular in patients affected from these mutations can be seen accumulation, in type-2 fibres, of highly ordered membrane tubules containing SR proteins, such as CASQ1, SERCA, triadin, RyR1, and STIM1. (Silva-Rojas R., et al. 2020).

Tubular aggregate myopathy is due to heterozygous mutations in STIM1 or ORAI1, while heterozygous mutations in CASQ1 have been found in patients with an exclusively muscular phenotype. All three genes encode key regulators of Ca^{2+} homeostasis, and thus act on a multitude of calcium-dependent cellular pathways, including muscle contraction.

Mutations involving STIM1 are present mainly in the Ca^{2+} binding EF domain: this induces constitutive unfolding and constitutive oligomerization of the protein. This suggests that mutations in the EF domain directly or indirectly impact Ca^{2+} coordination or destabilize the interaction between the EF and SAM domains, and

thus cause unfolding and oligomerization of STIM1, and consequently activation of the ORAI1 Ca^{2+} channel without prior depletion of Ca^{2+} stores.

In addition, six different missense heterozygous mutations were found in ORAI1 in patients with TAM/Stormorken syndrome and all of them involve highly conserved amino acids in transmembrane domains.

Mutations in ORAI1 do not significantly alter the localization of ORAI1 in the plasma membrane or the recruitment of ORAI1 with STIM1 oligomers but result in a basal increase in Ca^{2+} and excessive influx into the cell. (Böhm and Laporte, 2018)

Concerning CASQ1, three mutations, p.Asp44Asn, p.Gly103Asp, and p.Ile385Thr have been identified in patient with TAM. Every patient experienced slightly different symptoms and histopathological findings.

There is another mutation in CASQ1, p.Asp244Gly, related to a different myopathy.

It is defined as vacuolar myopathy, a mild myopathy accompanied by muscle cramping, reduced muscle strength, fatigue, and elevated plasma creatine kinase (CK) levels. Also, it is known the presence, mainly in type II fibres, of vacuoles that does not stain by routine histochemical analysis and contain aggregates of SR protein.

The mutation affects a conserved high-affinity Ca^{2+} binding sites of CASQ1 and alters the kinetics of CASQ1 polymerization and Ca^{2+} release in muscle fibres and primary myotubes. In particular, CASQ1 p.Asp244Gly forms large aggregates, with atypical dimer interactions.

Similar to the p.Asp244Gly mutation, alteration of CASQ1 polymerization is a typical trait of p.Asp44Asn, p.Gly103Asp, and p.Ile385Thr mutations, resulting in a reduced ability to store Ca^{2+}.

CASQ1 mutations are also associated with altered SOCE. In particular, two of these mutations (p.Asp44Asn and p.Ile385Thr), expressed in non-muscle cells, were shown to have lost the ability to inhibit SOCE, while p.Gly103Asp mutation was still able to inhibit Ca^{2+} influx. (Barone et al, 2017)

CASQ1 p.Asp44Asn mutation is involved in the pathogenesis of a tubular aggregate myopathy characterized by muscle fatigue and diffuse exercise-induced myalgia.

This mutation is characterized by a decreased Ca^{2+} dependent polymerization leading to decreased Ca^{2+} binding ability and loss of SOCE inhibition.

Concerning CASQ1 p.Gly103Asp mutation, it is involved in a tubular aggregate myopathy with exercise-induced muscle pain, stiffness, and early fatigue.

This one also features a decreased Ca^{2+} dependent polymerization leading to decreased Ca^{2+} binding ability.

CASQ1 p.Ile385Thr mutation is involved in a tubular aggregate myopathy with myalgia and proximal muscle weakness. This mutation is characterized by moderately increased Ca^{2+} dependent polymerization leading to decreased Ca^{2+} binding ability and loss of SOCE inhibition. (Rossi *et al.*, 2021).

CASQ1 variant	**Ca^{2+}-dependent aggregation**	**Trypsin resistance**	**Contribution to Sarcoplasmic Reticulum Ca^{2+} storage**	**SOCE inhibition**
p.Asp44Asn	decreased	decreased	decreased	lost
p.Gly103Asp	decreased	decreased	decreased	maintained
p.Ile385Thr	moderately increased	maintained	decreased	lost

Table 1: Properties of the CASQ1 mutations p.Asp44Asn, p.Gly103Asp, p.Ile385Thr detected in patients with Tubular Aggregate Myopathy compared to those of wild-type CASQ1. (Barone, V, Del Re, V, Gamberucci, A, et al.,2017)

2.AIM OF THE STUDY

This research aims to study the interaction between Calsequestrin protein and the SOCE mechanism for Ca^{2+} intake in three mutants precedingly identified in patients affected by TAM (Barone V., et al, 2017).

Expression of CASQ1 mutations in eukaryotic cells revealed a reduced ability of all these CASQ1 mutants to store Ca^{2+} and a reduced inhibitory effect of p.Ile385Thr and p.Asp44Asn on store operated Ca^{2+} entry.

This work of thesis will focus on the expression of CASQ1 mutants in muscle cells of knockout mice and the study *ex vivo* of the mechanisms by which these mutations reduce Ca^{2+} uptake by skeletal muscle fibres, namely the reduction of SOCE activity and the reduction of intra-reticular Ca^{2+} storage.

To investigate the functionality of mutated CASQ1 a mouse model was developed using CASQ1 KO mice and expressing via transfection a gene construct containing the mutated CASQ1. These fibres were then tested both for total Ca^{2+} storage and SOCE activity, together with KO fibres and fibers transfected with WT CASQ1 as control.

Total ER Ca^{2+} concentration was measured using Fura-2 as a ratiometric indicator and a release cocktail; SOCE activity was measured using Manganese quenching technique.

Expression and localization of exogenous CASQ1 were measured through fluorescence confocal microscopy.

3- MATERIALS AND METHODS

3.1- ANIMALS

4–6 months old WT and CASQ1-null mice on congenic C57bl/6J background were housed in micro-isolator cages at 20°C in a 12h light/dark cycle and provided free access to standard chow and water.

3.2- PLASMID PREPARATION

To assess the impact of mutations in muscle cells we prepared FDB muscle fibres from mice WT and KO for CASQ1, with or without the transfection of WT or mutated CASQ1 via electroporation.
The process of preparation of plasmid and transfection inside the muscle was finely tuned during the preliminary phase of this project.
As plasmid vector was chosen pEGFP, replicated in *E. coli* X-Gold strain competent cells, stored at -80°C. After a controlled thaw in ice at 4°C, 1ng of plasmidic DNA is mixed with 40uL of competent cell solution at OD_{600}= 3. The solution rest for 60" then electrotrasformation is performed using BioRad Gene Pulser apparatus. Using an electrophoretic cell, the bacteria diluted in 1mL of LB medium (Luria Bertani) are exposed to a single impulse of 12.5 kV/cm for 4.5-5.0 msec. The settings are as manufacturer suggested: 25 uF and 200Ω. Immediately after the pulse 1mL of SOC medium (Super Optimal Broth) is added to the solution and bacteria rests 1h at 37°C.
Bacteria are then plated on Petri dish with selective medium (LB Agar + Kanamicin 45ug/mL) and stored at 37°C overnight.
After the growth, isolated colonies are selected and inoculated in LB broth overnight.
The plasmid is then purified from the culture first with a MiniPrep using ThermoFisher MiniPrep kit. The resultant DNA is stored at 4°C until use. This DNA is tested for plasmid concentration using a combination of electrophoresis and NanoDrop quantification to assess the ratio of plasmid DNA: chromosomic DNA.
If deemed sufficient a MaxiPrep is performed, using ThermoFisher MaxiPrep kit.

Then the plasmid is again quantified using NanoDrop. Accepted concentrations range from 1.1-1.2 ng/uL to 2-2.5ng/uL.
In the end two test are performed to confirm the correct preparation of plasmid.
First a simple transfection of Hela Cells using Lipofectamine 2000 kit from ThermoFisher, transfection was then confirmed using a confocal fluorescence microscope to search for GFP fluorescence.
Second test involved the use of restriction enzyme: this way verifying that the whole plasmid was correctly amplified: 1ng DNA is mixed with 1uL of restriction enzyme provided by Merck in the appropriate buffer.
Restriction reaction is then incubated at 37°C for 1 hour, then the digestion is stopped by heat inactivation (65°C for 15min) or addition of 10mM final concentration EDTA. Finally, the digested DNA is loaded in electrophoretic gel composed of 1% agarose and run at 5V, together with a ladder, until sufficient separation of the bands. DNA is stained with SYBR green and visualized using UV light.
Bands are confronted with mass ladder to verify that the plasmid of interested was amplified, knowing the expected mass of restricted DNA.
Once obtained, the plasmid DNA was stored at -20°C until use.

3.3 FDB MUSCLE TRANSFECTION

To perform transfection, mouse was first anesthetized with 3% isoflurane and then an injection of hyaluronidase (2 µg/ml) into FDB muscle was performed. After 1 hour the mouse was again anesthetized with 3% isoflurane after which 10 ng of plasmid DNA was injected.

After 15 minutes an electroporation with 20 pulses at 120W was performed in order to facilitate the entry of plasmid DNA into the nuclei. The subsequent isolation and analysis of fibres expressing the protein of interest is performed 10-12 days after electroporation.

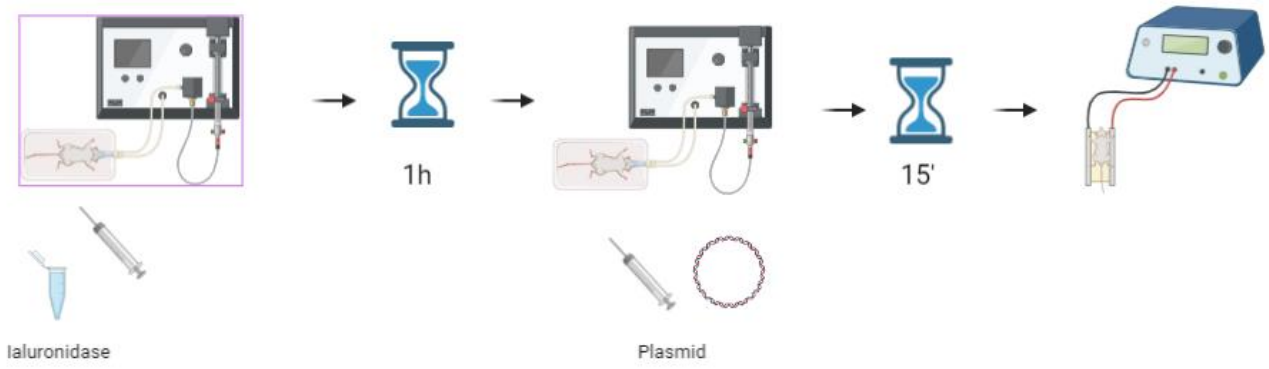

Figure 6: schematic representation of FDB muscle transfection process.

3.4 FDB FIBERS ISOLATION

Muscle fibres belonging to the FDB muscle were isolated from mice, which were previously anesthetized in a CO2-saturated chamber and subsequently sacrificed by cervical dislocation.

The muscle taken from the mouse paw was placed first in myorelaxant solution (KCl 0.1 M, EGTA 5mM, $MgCl_2$ 5mM, BTM 3mM, histidine 10mM, DTT 0.25 mM) for 10 min in ice and subsequently incubated at 37°C/5% CO_2 for 1 hour and 30 minutes in a Tyrode buffer solution (NaCl 134 mM, KCl 2.68 mM, $CaCl_2$ 1.8 mM, $MgCl_2$ 1.05 mM, NaH_2PO_4 0.417 mM, $NaHCO_3$ 11.9 mM, Glucose 5.56 mM, pH 7.4) + 0.2% Collagenase + 10% Fetal bovine serum (FBS): this solution was first filtered and then the sterile FBS was added to avoid loss of volume.

The sample in collagenase is shaken approximately every 15 minutes to help expose all the tissue to the solution. After 90min minutes the sample is digested, the waste is removed and three washes of 10 min each are performed (after changing solution the sample is stored in incubator 37°C/5% CO_2), with the following solutions:

- *Tyrode*
- *Tyrode,* 10%FBS
- *Tyrode,* 1% penicillin/streptomycin, 10% FBS

each time removing the waste of the previous wash.

At the end of the third and final wash, the fluid containing the muscle is then moved in a sterile plate. Fibres are isolated by mechanical disaggregation with a 1ml serological pipette, then 1ml Gilson pipette with blunted tip to avoid damaging the fibres, and lastly with 200uL Gilson pipette with blunted tip as well. After that, tendons and skin remnants are removed using two tweezers.

Subsequently, fibres are homogeneously plated on Lab Tek™ II four-well plates cover glass previously treated with laminin 25 µg/ml o/n in 37°C.

The fibres are then stored in an incubator at 37°C/5% CO_2 and analysed within 24 hours but not first than 2h to let fibres adhere to laminin coat.

3.5 MEASUREMENT OF CALCIUM RETICULAR STORES

To evaluate the function of CASQ1 in its role as a buffer of reticular Ca^{2+} we performed measurement of total Ca^{2+} stores of the sarcoplasmic reticulum in the muscle fibres isolated from CASQ1 WT mice, CASQ1 KO mice (and CASQ-KO mice transfected with CASQ1 WT , CASQ1 p.Asp44Asn, CASQ1 p.Gly103Asp and CASQ1 p.Ile385Thr mutants Cytosolic transient Ca^{2+} was assessed by using the ratiometric fluorescent Ca^{2+} indicator Fura-2. In its esterified (acetoxymethyl-ester) and lipophilic (Fura-2 AM) form it penetrates the cell, where thanks to the action of cytosolic esterases that cut the AM group is trapped in the cytoplasm.

In this protocol, the fluorescence of Fura-2 is measured using the fluorescence microscope (Nikon ECLIPSE TE300), at the excitation wavelengths of 340 nm (calcium-bound Fura-2) and 380 nm (free, non-calcium-bound Fura-2). The ratio (R) of fluorescence intensity at $\frac{\lambda 340}{\lambda 380}$ is directly propoprtional to the level of Ca^{2+} in the cytoplasm and that, following treatment with a reticular Ca^{2+} depletion cocktail, applied in the absence of external Ca^{2+}, will give an increase in the signal that is proportional to the Ca^{2+} released from the sarcoplasmic reticulum.

To measure cytoplasmic Ca^{2+}, fibres are "loaded" for 30 min (at 37°C/5% CO_2) in a medium composed of *Ringer solution* (145 mM NaCl, 5mM KCl, 1mM $MgCl_2$, pH 7,4) containing 2mM Ca^{2+}, Fura-2 AM 5 µM and 1% BSA.

After 30 min, the solution with Fura-2 AM is removed and hydrolases are free to act for de-esterification of Fura-2 AM by changing solution with Ringer solution containing 2 mM Ca^{2+} (same solution as before but without Fura-2 AM) for 20 min in an incubator (37°C/5% CO_2).

Next, the Lab Tek™ with the fibres are placed on the microscope stage and the Ringer solution containing 2mM Ca^{2+} is replaced with a "Calcium Free Ringer solution" (containing 0.2 mM EGTA) to measure basal Ca^{2+} levels in the cytoplasm and the signal changes (ratio 340/380) that follow depletion of the reticular stores.

All the buffer including the calcium free ringer solution that were used while fibres are

under the microscope are heated by a thermostatic bath at 37°C to avoid heat stress and help maintaining a good health of the fibres during observation.
In order to induce the release of all reticular Ca^{2+}, fibres where then exposed to a "depletion cocktail" composed by ionomycin 10 µM (ionophore for Ca^{2+}) and CPA 30 µM (SERCA inhibitor) in Calcium Free Ringer solution, all while measuring the signal at 340nm and 380nm.
To assess the extent of Ca^{2+} stores, the "Area Under the Curve" AUC is calculated in the 6 minutes following the use of depletion cocktail.
Altogether, including the baseline measurement and standard time to change the media, no observation was carried out for less than 10' to standardize the curves.

3.6 CALCIUM INFLUX MEASUREMENT

To investigate whether or not the mutations in CASQ1 could impair the physiological function of SOCE, or the constitutive Ca^{2+} influx, we decided to compare the activation of (SOCE) Ca^{2+} influx in rest conditions both in WT, KO and KO transfected fibres with WT or mutated CASQ1.
To do so we used the validated method of "manganese quenching".

Fibres isolated in LabTek plates coated with laminin are loaded with Fura-2AM 5uM in a Ringer solution (145 mM NaCl, 5 mM KCl, 1 mM MgCl2, pH 7,4) with Ca^{2+} 2mM and 1% BSA to help Fura-2AM dilute. Loading phase is carried at 37°C/5% CO2 for 30min, then as described before medium is changed in a Ringer solution with Ca^{2+} 2mM but without Fura.

Then plates are put under microscope for the measurement. In manganese quenching what is measured is the "quenching" of Fura fluorescence thanks to the action of Manganese. Manganese binds Fura with higher affinity than Calcium, quenching the fluorescence. Also, the Manganese share the same ways to enter the cells as Ca^{2+}, and notably is also transported by the SOCE mechanism. Thus, measuring the velocity of the

quenching of fluorescence we have a direct correlation with the entry of Manganese which is directly correlated with SOCE activation. Confronting these velocity (measured as the slope of the curve of fluorescence quenching) between the transfected fibres, WT and KO we have the possibility of assessing the mutation influence on the mechanism.

To measure the quenching medium is firstly changed in a Ringer solution without Ca^{2+} but containing EGTA 0.2mM, then basal levels of fluorescence are measured. After a while Manganese 0.5mM (final concentration) is added to the medium, and the curve of Fura fluorescence is closely measured to then calculate the slope. We used for fluorescence measurements Nikon ECLIPSE TE300 fluorescence microscope, and we measured the fluorescence at 360nm, that is the isosbestic point of Fura, to avoid interference from Ca^{2+} free/bound.

3.7 NORMALIZATION AND STATISTICS

Because the observation of Fura-2 signal (both 340/380nm ratio for calcium storage and 360nm for manganese quenching) is an indirect measurement, great care has been took in standardize the measurements between different fibres.

First of all, we confirmed that there was no significant difference in different mouse transfected with the same mutation.
We also tested if there was significant difference between "naïve" KO mice and KO mice electroporated with water to simulate the "blank" of plasmid. There was no mathematical significance between the two groups but, because there was some difference appreciable, we decided to use as control KO mice electroporated with a water.
Also the time intercourse between electroporation and FDB fibres isolation was carefully selected to let the tissue recover from the insult, but without starting to lose the expression of exogenous protein. After testing 3, 7, 10, 12 and 20 days from electroporation we decided to pick between 10 and 12 days from the procedure as our timeframe, where we found that no damage was visible in the muscle and the expression was still strong.

To normalize the curves of fluorescence, we carefully choose a time (6') where most of the curves had "exhaust" all the stimulus, to even the field between different fibres that could react faster or slower.
Also we decided to put a limit on the diameter of fibres to measure, because we noted that high diameter fibres had a noticeable slower response than the others.

We recorded baseline level for at least 2' every time to then normalize, subtracting the slope from normal bleaching of the fluorophore or other interference.

Finally all the fibres were treated between 24h from isolation, and if the LabTek plates started to show sign of stress (due to temperature shock or other causes) those fibres were not taken into account.

Statistical analyses were made using t-student test with Welsch correction (due to different SD between group), all confronting single mutations versus CASQ1$^{KO/WT}$, our "recovered" WT that was choose as control due to the more precise confrontation with other exogenous protein expression.

4.RESULTS

4.1 TRANSFECTED CASQ1 IS CORRECTLY EXPRESSED IN FDB FIBERS

As can be seen from **Figure 7**, transfection of plasmid DNA leads to expression of CASQ1 throughout the fibre, with a pattern that is compatible with junctional reticulum localization.

The zoomed image obtained by confocal microscopy show staining with different antibodies in a fibre transfected with CASQ1^{Ile385Thr} -GFP where we can see the calsequestrin correctly localized in terminal cisternae, identified by the co-staining with RYR1 and α-actinin.

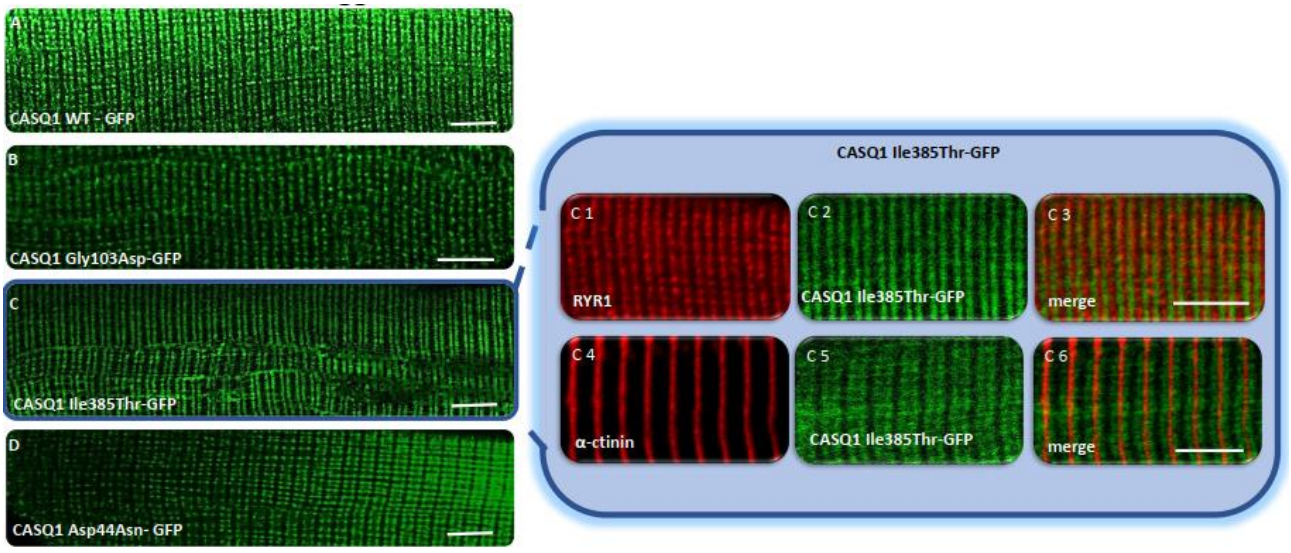

Figure 7: Representative FDB muscle fibres isolated and cultured from CASQ1^{KO} mice transfected with CASQ1 ^{WT}-GFP (**A**), CASQ1 ^{Gly103Asp} –GFP (**B**), CASQ1 ^{Ile385Th}r– GFP (**C**), CASQ ^{Asp44Asn} – GFP (**D**). In C 1-6 representative images of FDB fibres from CASQ1 ^{KO} mice expressing CASQ1 Ile385Thr–GFP and stained with anti-RYR1 (**C1**) and α-ctinin antibodies (**C4**); C3 and C6: merged images. Scale bar 5 μm.

In some perinuclear regions, large intensely stained aggregates, due to overexpression of calsequestrin, can be seen. Microscopic observation of the signal CASQ1-GFP is necessary to select regions where to measure the fluorescence of Fura-2 in fibres and avoid areas where GFP it is overexpressed or not expressed at all.

4.2 TRANSFECTION CAN RESTORE CALCIUM BUFFERING ABILITY IN KO FIBERS

To measure reticular Ca^{2+} stores, FDB fibres are loaded with Fura-2, as described in paragraph 3.5, then, by single-cell measurement under a fluorescence microscope, the signal of the ratio 340/380 was recorded for at least 10', allowing to measure changes in cytosolic Ca^{2+}.

The fibres are placed in "Calcium-Free Ringer solution". Initially the cytosolic basal Ca^{2+} level is measured and subsequently depletion of the sarcoplasmic reticulum is induced with the depletion solution.

A release curve is thus obtained and the AUC ("Area Under Curve") is calculated in 6'. The AUC value is directly proportional to the content of reticular Ca^{2+} stores as, since there is no contribution of Ca^{2+} from outside, only the stocks contribute to this increase.

Regarding fibres belonging to WT mice, the obtained release curve represents the physiological situation of reticular Ca^{2+} stores.

Comparing the fibres belonging to electroporated WT mice with those belonging to electroporated KO mice (**Fig.8**), we observe that the latter present a very low AUC: this is explained because, given the absence of calsequestrin, Ca^{2+} is not stored in the reticulum and therefore does not result in a detectable concentration in the cytoplasm after depletion with ionomycin and CPA.

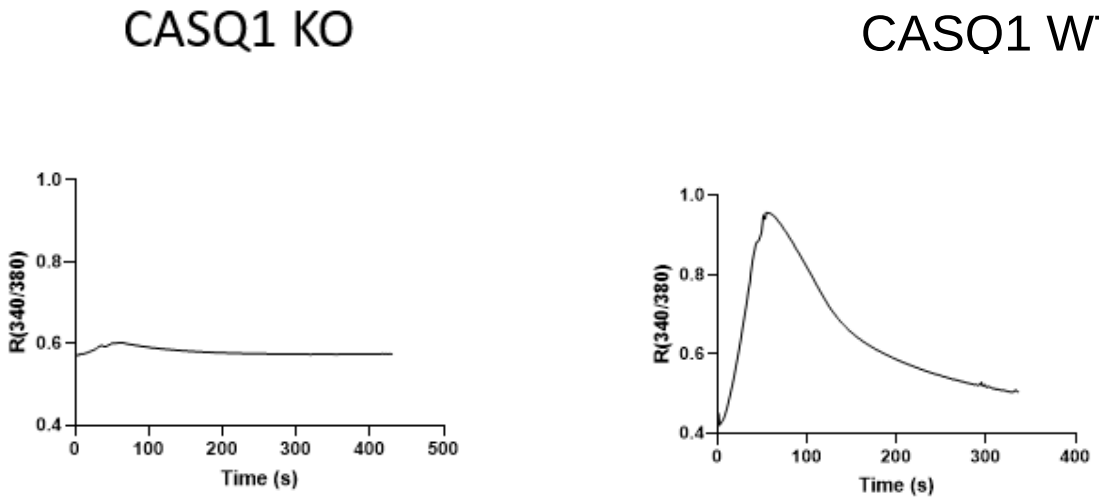

Figure 8: Representative traces of calcium reticular stores measurement after application of the depletion cocktail in FDB fibres obtained from CASQ1 ^{KO} and CASQ1 ^{WT} mice.

In addition to CASQ1^{KO} mice and CASQ1^{WT} mice, Ca^{2+} content is also assessed in the sarcoplasmic reticulum of KO mice transfected with GFP CASQ1 WT ("recovered" KO, CASQ1 $^{KO/WT}$).

Fibres from "recovered" KO mice restored, although not completely, reticular Ca^{2+} stores by showing a significantly higher AUC than the KO sample (**Fig.9**).

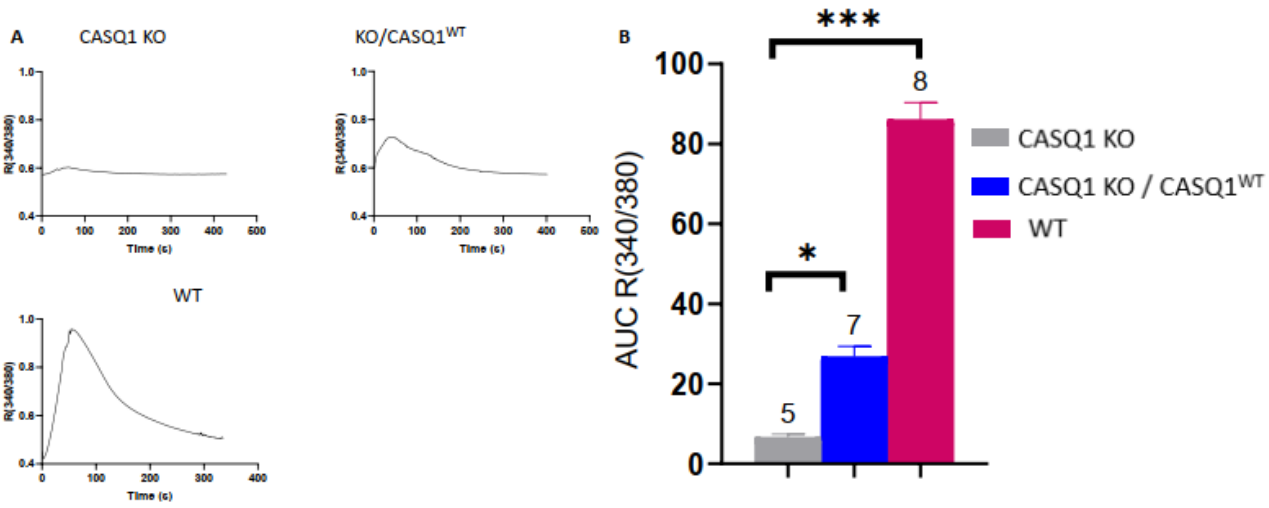

Figure 9: Representative curves of FDB fibres from CASQ1 ^{WT}, CASQ1 ^{KO} and CASQ1 ^{KO} transfected with CASQ1-^{WT} mice, treated with Ca^{2+} release cocktail (A). AUC of Fura-2 fluorescence from CASQ1 ^{WT}, CASQ1 ^{KO} and $^{KO/WT}$ fibres (B). Bars as mean with SEM, numbers on bars indicates sample size. P values ≤0.05 and 0.001 are indicated by * and *** respectively.

As a control, fibres belonging to "recovered" KO mice were used, in order to simulate both electroporation and plasmid expression conditions.

4.3 RETICULAR CALCIUM CONTENT IS REDUCED IN CASQ1 MUTANTS

After validating the CASQ1^{KO}/^{WT} "recovered" mouse as positive control Ca^{2+} content in the sarcoplasmic reticulum was then evaluated in CASQ1^{Asp44Asn}, CASQ1 ^{Gly103Asp} and CASQ1 ^{Ile385Thr} mutants.

Previous experiments on cells have illustrated the following results (**Fig.10**) for the three mutations associated to TAM:

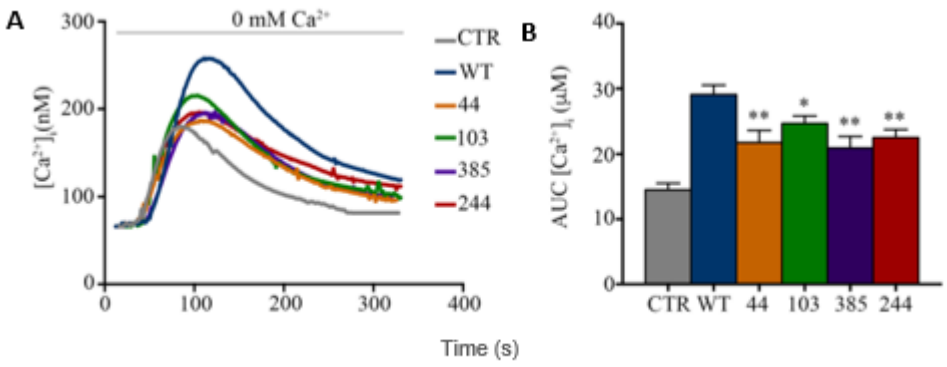

Figure 10: Representative traces of Ca^{2+} release from intracellular stores of cells untransfected (CTR) or transfected with WT or different CASQ1 mutations (**A**); Results of measurement of calcium reticular stores (AUC) transfected HeLa cells (**B**) (Barone, V, Del Re, V, Gamberucci, A, et al.,2017).

$CASQ1^{Asp44Asn}$, $CASQ1^{Gly103Asp}$ and $CASQ1^{Ile385Thr}$. A further mutation, $CASQ1^{Asp244Gly}$, is reported, which is not isolated from TAM patients, but from patients with vacuolar myopathy.

All four mutations reveal a decrease in sarcoplasmic reticulum Ca^{2+} storage. In cell experiments.

Following these results on cells, we evaluate how, the same mutations, behaves in fibres *in vivo*.

To assess this, as already explained in Chapter 3, we initially transfected $CASQ1^{KO}$ mice with the previously prepared plasmid. Subsequently, it is electroporated and, only after 10-12 days, the fibres are isolated and analysed.

The analysis consists of measuring basal Ca^{2+} levels in the cytoplasm and Fura signal (340/380 ratio) that follow depletion of reticular reserves: this allows us to evaluate the entity of the Ca^{2+} reserves simply by calculating the AUC following the use of depletion cocktail, to standardize the measurement we recorded the signal for 6' after the depletion cocktail exposure.

The results obtained were then grouped and plotted in a graphic (**Fig.11**).

Figure 11 presents the results of AUC in 6' relative to $CASQ1^{KO}$ mice, "recovered" KO mice ($CASQ1^{KO/WT}$), $CASQ1^{Asp44Asn}$, $CASQ1^{Gly103Asp}$ and $CASQ1^{Ile385Thr}$ mutants.

Overall, results of AUC in 6' showed a decrease in sarcoplasmic reticulum Ca^{2+} storage in all three tested mutants, compared to $CASQ1^{KO/WT}$.

A remarkable decrease of the sarcoplasmic reticulum Ca^{2+} storage was observed for $CASQ1^{Ile385Thr}$ and $CASQ1^{Asp44Asn}$ mutants, these mutations showed a significant decrease, with values of AUC much closer to $CASQ1^{KO}$ than $CASQ1^{KO/WT}$.

Less severe effects are observed in $CASQ1^{Gly103Asp}$ mutant, where is appreciable a decrease of around 30% but without statistical significance, mainly due to the fact that standard deviation is high in all groups.

The difference between $CASQ1^{Asp44Asn}$/$CASQ1^{Ile385Thr}$ and $CASQ1^{KO/WT}$ is high enough to easily assess statistical significance.

The significance value was calculated with student-t test with Welsch correction, comparing every mutant with $CASQ1^{KO/WT}$.

Considering these results, we can compare what happens in HeLa cells (**Fig. 10B**) with our *ex vivo* experiments: differences in fibres are harder to highlight compared to cells due to the complexity of the procedure, involving both electroporation and single fibre isolation and analysis.

Nonetheless, we can see similar scenario between the two sets of results with general severity of the mutation comparable both in cells and fibres.

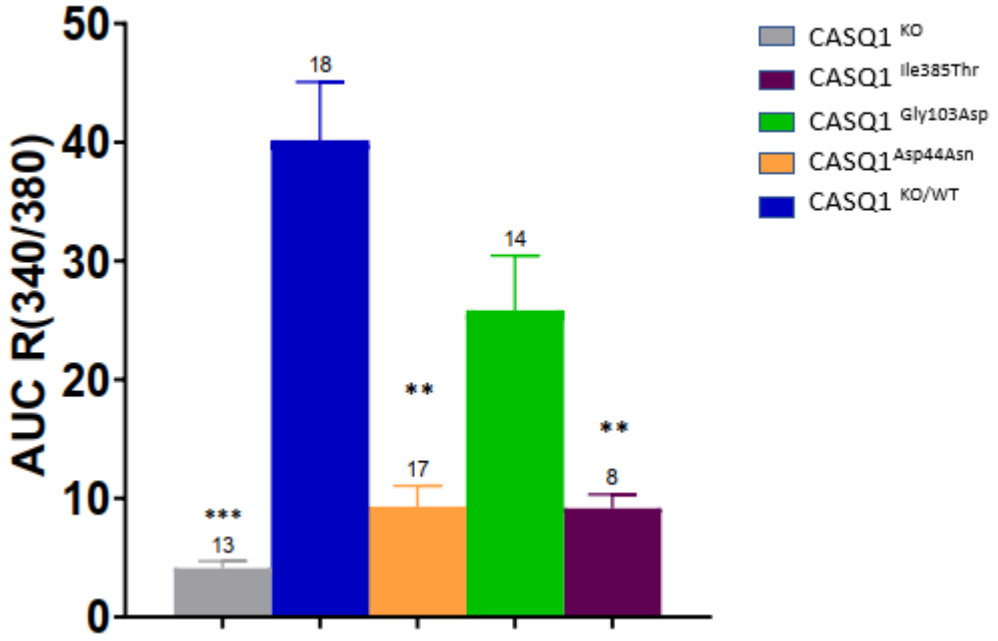

Figure 11: Results of measurement of calcium reticular stores (AUC) in FDB from mice electroporated with the indicated mutations. Numbers on bars indicate the fibres tested for each sample. Bars are mean ±SEM. **, P≤0.01; ***, P≤0.001.

4.4 MUTATIONS SUPPRESS CASQ1 INHIBITION OF SOCE

Figure 12 shows the effects of CASQ1 in the activation of SOCE in HeLa (non-muscle) cells and in particular in non-transfected cells (CTR), transfected with WT or with mutant CASQ1. Expression of the $CASQ1^{Asp44Asn}$ and $CASQ1^{Ile385Thr}$ mutations did not lead to a significant reduction in Ca^{2+} influx, suggesting a reduced ability to inhibit SOCE. In contrast, expression of the $CASQ1^{Gly103Asp}$ mutation resulted in an inhibition of Ca^{2+} influx comparable to that obtained with $CASQ1^{WT}$. A further mutation, $CASQ1^{Asp244Gly}$, is reported, which is not isolated from TAM patients, but from patients with vacuolar myopathy. This mutation doesn't show effects on SOCE whatsoever.

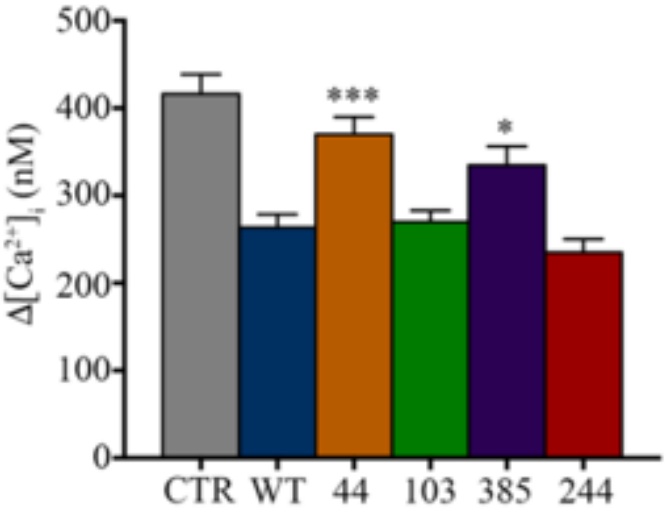

Figure 12: Quantification of Ca^{2+} influx in HeLa cells expressing WT and mutant CASQ1. Bars indicate $\Delta[Ca^{2+}]I$ (nM) ± SEM. (Barone, V, Del Re, V, Gamberucci, A, et al.,2017)

To evaluate SOCE activity in fibres we used manganese quenching technique, subtracting the slope of pre-Manganese exposure (derived from natural bleaching of Fura) from the slope post-Manganese, thus obtaining the kinetics of SOCE channels throughout the fibres. Fibres were kept in a Ca^{2+} rich environment before the exposure to Manganese, to be able to assess the rest condition activation of SOCE. We made also some preliminary calibration experiments using the same depletion cocktail that we already described on fibres WT and KO before measuring the manganese quenching, and as can be seen in **Figure 13** the effect was similarly

visible both in depleted and "rest" condition, representing store-operated and constitutive Ca^{2+}-entry. This led us to decide to work with non-depleted fibres to analyze the constitutively active Ca^{2+} entry that provides a continuous flow of Ca^{2+} in absence of the buffering ability of CASQ1.

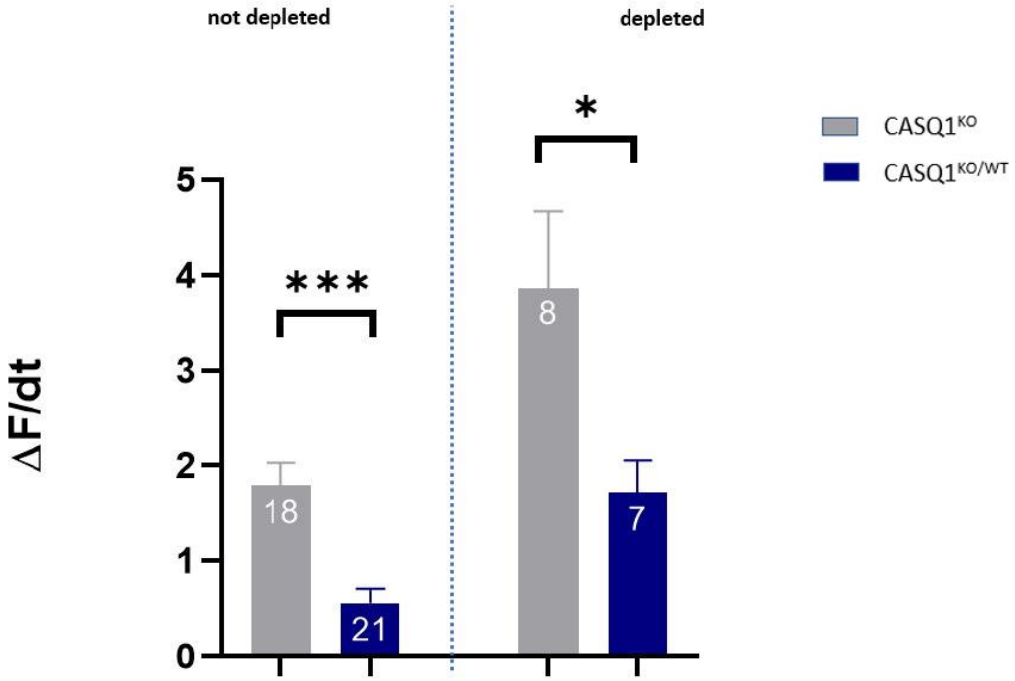

Figure 13: Quantification of Mn influx in isolated fibres from CASQ1^{KO} and CASQ1 $^{KO/WT}$ mice, depleted or not with ionomycin 10 µM and CPA 30 µM in Calcium Free Ringer solution. Bars as mean± SEM. **, P≤0.01; ***, P≤0.001.

The data shown in **Fig 14** are derived from ex vivo analyses performed on FDBs isolated from three main models: CASQ1^{KO}, CASQ1$^{KO/WT}$ and CASQ1^{KO} transfected with CASQ1 mutants.

From the data shown in **Figure 14** the fibres obtained from the CASQ1^{KO} mice have very high constitutive influx kinetics (ΔF/dt ≈ 1.8) as evidenced by the corresponding column height. This could be motivated by the absence of calsequestrin, which cannot exert its inhibition mechanism on STIM1.

CASQ1 $^{KO/WT}$ fibres and fibres derived from mutant CASQ1 behave differently, all showing lower levels of SOCE activation in respect to CASQ1^{KO}.

CASQ1^{KO} show an important constitutive Ca^{2+} influx even in rest condition, as concordant with bibliography and cells data, but is also very measurable the high Ca^{2+} influx even in rest condition in all the mutants transfected fibres.

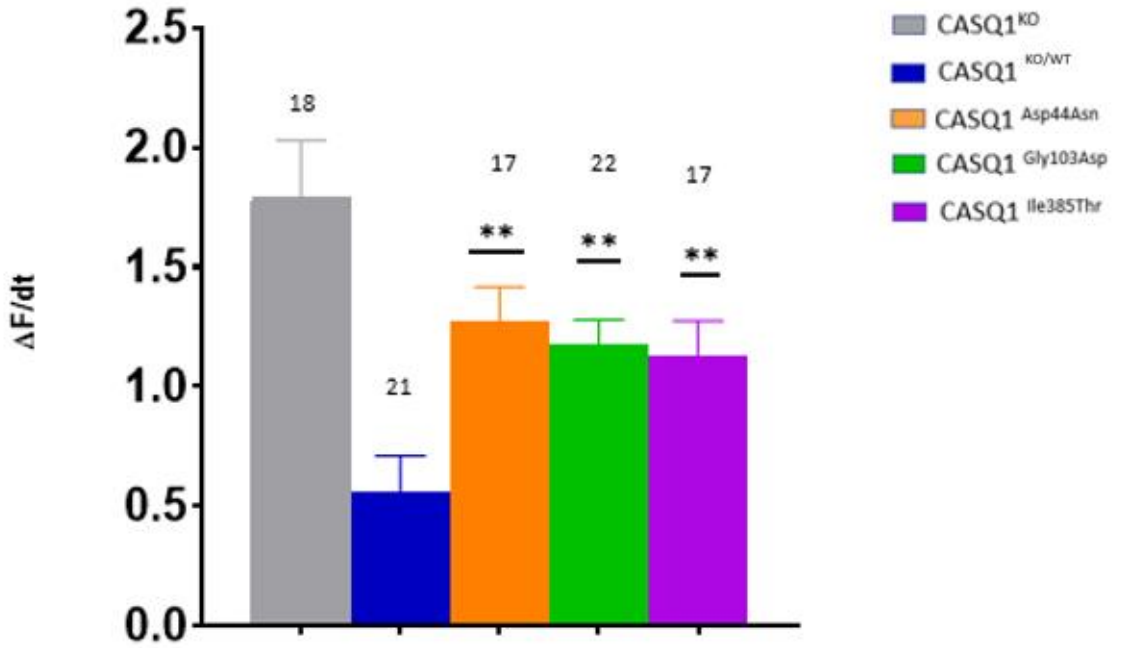

Figure 14: Quantification of Mn influx in isolated fibres from CASQ1^{KO}, CASQ1 $^{KO/WT}$, CASQ1^{Asp44Asn}, CASQ1^{Gly103Asp} and CASQ1^{Ile385Thr} mice. Bars as mean± SEM. **, P≤0.01.

Contrary to the cell data, in our model all three mutations showed high constitutive influx of Ca^{2+}, without appreciable differences between them, and an estimated difference of around 30% between the CASQ1^{KO} influx and the mutants influx.
CASQ1^{Asp44Asn} registering a little higher results than the other two, and notably this mutations was also the harder to culture, with fibres very fragile due to the formation of "cloths" of calsequestrin in some of the fibres, that were then not eligible for observation.

5. DISCUSSION

CASQ1 is a protein that has been known since its discovery 50 years ago in rabbit skeletal muscle (MacLennan, D. H. & Wong, P. T.,1971). The cDNA of CASQ1 was cloned from fast-twitch skeletal muscle from rabbits, and the cDNA of the cardiac isoform of CASQ (CASQ2) was cloned from the heart and slow-twitch skeletal muscle from canines. CASQ1 is the major isoform in adult fast-twitch skeletal muscles, while CASQ2 is the only isoform in cardiac muscle and a minor isoform in adult slow-twitch skeletal muscle. Smooth muscle expresses both isoforms.

CASQ1 and CASQ2 are heavily enriched in the SR, and they are tightly associated with the membrane of JSRs but not LSRs (in the case of rabbit CASQ1, approximately 70% after a purification process). CASQs are not evenly distributed in the SR but are concentrated in the vicinity of what were recently defined Calcium Entry Unit (CEU) (Michelucci A, 2020). The first role of CASQ1 in skeletal muscle is to buffer Ca^{2+} in the SR with a low-affinity and high-capacity Ca^{2+}-binding ability (40–50 moles or maximally ~80 moles of Ca^{2+}/1 mole of CASQ1) to prepare rapidly releasable Ca^{2+} during EC coupling. Ca^{2+}-binding sites in CASQ1 are very different from those in other Ca^{2+}-binding proteins (i.e., they do not consist of EF-hands). The role of CASQ1 as a high-capacity Ca^{2+}-buffering protein is accomplished by two factors. First, CASQ1 is an extremely acidic protein. Two-thirds of the C-terminus of CASQ1 is negatively charged, and it serves as the Ca^{2+}-binding site. Second, CASQ1 self-polymerizes to prepare high-capacity Ca^{2+}-binding at high [Ca^{2+}] in the SR (He, Z., et al. ,1993).

In most cell types, the Ca^{2+} gradient between the cytosol (approximately 100 nM) and extracellular space (mM range) is maintained (approximately 20,000-fold), which suggests that extracellular Ca^{2+} is an effective source of intracellular Ca^{2+} signals. SOCE is one extracellular Ca^{2+} entry route in various cells. Generally, SOCE is operated by coordinated interactions between STIMs (STIM1, STIM1L, and STIM2) and Ca^{2+} release activated Ca^{2+} channel proteins (Orai1, Orai2, and Orai3). STIM1 and Orai1 are the major isoforms mediating SOCE. STIM1 in the ER membrane senses the depletion of Ca^{2+} from the ER via its EF-hand motif, and it activates Orai1 in the plasma membrane via a physical interaction between the cytoplasmic C-terminus of STIM1 and the STIM-Orai1-activating region (SOAR) of Orai1. During this process, sensing Ca^{2+} by STIM1 (i.e., Ca^{2+} depletion from the ER) induces the homo-oligomerization of STIM1 and its relocalization to the ER membrane

near the plasma membrane where Orai1 is located, which also induces the homo-oligomerization of Orai1. The final hetero-oligomers that are formed by STIM1s and Orai1s are called '*puncta*'.

The other main role of CASQ1 in skeletal muscle is as a regulator of SOCE via physical interaction between STIM1 and the acidic asp-rich/CAS region of CASQ1. Overexpression of CASQ1 in C2C12 myotubes inhibits SOCE, while SOCE is increased in FDB skeletal muscle fibres from CASQ1 single- or CASQ1/CASQ2 double-knockout mice (Yarotskyy, V., Protasi, F. & Dirksen, R. T., 2013). Therefore, CASQ1 not only modulates intracellular Ca2+ release but also provides a "reverse-directional signal" to regulate SOCE in skeletal muscle (a signal in the opposite direction of the orthograde signal from DHPR in the t-tubule membrane to RyR1 in the SR membrane during EC coupling, i.e., a signal from CASQ1 in the SR to Orai1 in the t-tubule/plasma membrane) suggesting that the functional interplay among CASQ1, RyR1 and SOCE could also contribute to pathological Ca^{2+} overload as well as to physiological Ca^{2+} signals (Jin Seok Woo, et al. 2020)

Indeed this study have his roots in the discovery of CASQ1 mutations in Tubular Aggregates myopathy patients, in particular three mutations have been identified, that we have then investigated in this work: p.Asp44Asn, p.Gly103Asp, and p.Ile385Thr were all already transfected in eukaryotic cells and tested for SOCE regulation and total Ca^{2+} storage.
Results in cells showed a reduction of storage in all three mutants and a reduction of SOCE regulation (and thus an hyperactivation of SOCE) in 2 of the mutants tested, namely p.Asp44Asn and p.Ile385Thr.

As already discussed we started testing the expression of mutants in transfected FDB fibres, using a confocal microscope to confirm the correct localization.
Indeed has been proven (Michelucci, A. 2020) that CASQ1 KO mice have smaller terminal cisternae, suggesting an "inductor" mechanism of CASQ1 in the development of this reticular district, but nonetheless, taking care of loading the correct amount of DNA and waiting for the inflammation following the electroporation to resolve, the localization of

CASQ1 in our fibre was very good, and also the expression was homogeneous to have a distribution of the protein all along the fibres.
In early stage of assessing the protocol we found higher concentrations of proteins near the nuclei, sometimes forming a sort of precipitation or molecular aggregates, that could resemble the ones from patients affected by tubular aggregates myopathies, even if in cellular scale. Scaling back the quantity of DNA transfected, choosing younger mice and letting the muscle rest longer after the electroporation have sensibly reduced the insurgence of such hyperexpression.

The first function of CASQ1 that we wanted to test in mutants was the buffering of Ca^{2+} in the reticulum.
From HeLa cells experiment we already knew that all three mutations showed lower Ca^{2+} storage in transfected cells, so after validating our control ($CASQ1^{KO/WT}$) we proceed to investigate the three mutations impact on FDB fibres.

In a different fashion from cells experiment, CASQ1 ^{Gly103Asp} did not registered a significant difference with $CASQ1^{KO/WT}$, even if the total Ca^{2+} storage from this mutation was still considerably higher than $CASQ1^{KO}$.
The other two mutations, CASQ1 ^{Asp44Asn} and CASQ1 ^{Ile385Thr} both had the ability to restore some form of "stocks" of Ca^{2+}, compared to $CASQ1^{KO}$ their signals were close to double, but with more than significant differences in regard to the stocks of $CASQ1^{WT}$.

So we can affirm that CASQ1 ^{Asp44Asn} and CASQ1 ^{Ile385Thr} mutations impairs the ability of CASQ1 to act as a buffer of Ca^{2+}, losing is ability to store large amounts of ions as it should be. This alone could explain some of the symptoms like myalgia and weakness that TAM patients experience, due to the lower Ca^{2+} stocks, repetitive muscle contraction is not easily achievable. Even if $CASQ1^{KO}$ models are known to employ some adaptation for the loss of Ca^{2+} storage, namely the CEUs described in paragraph 1.4, there is no doubt that also CASQ1 ^{Asp44Asn} and CASQ1 ^{Ile385Thr} as $CASQ1^{KO}$ are not able to stock Ca^{2+} in the sarcoplasmic reticulum as CASQ1 "functional" genotypes can.
The existence of CEUs provides indeed a possibility for the sarcoplasmic reticulum to retain is function thanks to the high Ca^{2+} influx that a similar cytological organization can

generate, helping to overcome this inability of stocking Ca^{2+}. In future experiments should be investigated whether a genotype CASQ1 ^{Asp44Asn} or CASQ1 ^{Ile385Thr} mouse have constitutive formation of CEUs in their muscle fibres as the CASQ1^{KO} mouse.

At last, we investigated the other main role of CASQ1 as regulator of SOCE, as already stated the loss of SOCE inhibition can lead to pathological Ca^{2+} overloads, leading to impair in the EC-coupling mechanism, loss of plasma membrane polarization and cell death.
In cellular experiments these three mutations had heterogeneous results, CASQ1^{Asp44Asn} and CASQ1^{Ile385Thr} mutations were not able to reduce Ca^{2+} influx, suggesting an inability to inhibit SOCE. In contrast, expression of the CASQ1^{Gly103Asp} mutation resulted in an inhibition of Ca^{2+} influx comparable to that obtained with CASQ1^{WT}. Moving to fibres experiments again we had slightly different results.

In FDB fibres isolated from all three mutations: CASQ1^{Asp44Asn}, CASQ1^{Ile385Thr}, CASQ1^{Gly103Asp} an high constitutive Ca^{2+} influx was measured even in rest condition. Fibres were kept in a Ca^{2+} rich environment (Ca^{2+} 2mM) until the very moment when the medium changed in Ringer solution with EGTA to assess baseline signal before the addition of Manganese to the extracellular medium.
Nonetheless all three mutations, and with a slightly higher kinetic CASQ1^{KO}, had a stable and significant influx of Manganese that quenched the fluorescence of Fura. Manganese is transported by the SOCE mechanism to enter the cell, confirms that in all 4 of those models (CASQ1^{KO}, CASQ1^{Asp44Asn}, CASQ1^{Ile385Thr} and CASQ1^{Gly103Asp}) there was no "breaking" action of CASQ1 on SOCE, and possibly on STIM1.

These 3 mutations, regarding the ability of CASQ1 to regulate SOCE, can very well be considered loss of function.

We hope that this work could help linking CASQ1 as another actor in TAM pathophysiology, but further studies must be conducted to investigate the mechanism behind this loss of function.

Also, the measurements of intracellular of intrareticular movements of ions is not an easy task but recently many innovations in this field are being developed, together with new methods to culture myotubes and simulate more finely the physiological environment of muscle. More experiments using new techniques and machines are to be done to properly link these mutations to SOCE and TA myopathy, and to confirm these multiple roles of CASQ1, much more than a simple buffering protein.

6. BIBLIOGRAPHY

- Avila, G. *et al.* (2019) 'Ca^{2+} Channels Mediate Bidirectional Signaling between Sarcolemma and Sarcoplasmic Reticulum in Muscle Cells', *Cells*. NLM (Medline). Available at: https://doi.org/10.3390/cells9010055.

- Avila, G. *et al.* (2020) 'Ca^{2+} channels mediate bidirectional signaling between sarcolemma and sarcoplasmic reticulum in muscle cells', *Cells*. MDPI. Available at: https://doi.org/10.3390/cells9010055.

- Barone, V. *et al.* (2017) 'Identification and characterization of three novel mutations in the CASQ1 gene in four patients with tubular aggregate myopathy', *Human Mutation*, 38(12), pp. 1761–1773. Available at: https://doi.org/10.1002/humu.23338.

- Beard, N.A., Laver, D.R. and Dulhunty, A.F. (2004a) 'Calsequestrin and the calcium release channel of skeletal and cardiac muscle', *Progress in Biophysics and Molecular Biology*, pp. 33–69. Available at: https://doi.org/10.1016/j.pbiomolbio.2003.07.001.

- Beard, N.A., Laver, D.R. and Dulhunty, A.F. (2004b) 'Calsequestrin and the calcium release channel of skeletal and cardiac muscle', *Progress in Biophysics and Molecular Biology*, pp. 33–69. Available at: https://doi.org/10.1016/j.pbiomolbio.2003.07.001.

- Böhm, J. and Laporte, J. (2018a) 'Gain-of-function mutations in STIM1 and ORAI1 causing tubular aggregate myopathy and Stormorken syndrome', *Cell Calcium*. Elsevier Ltd, pp. 1–9. Available at: https://doi.org/10.1016/j.ceca.2018.07.008.

- Böhm, J. and Laporte, J. (2018b) 'Tubular aggregate myopathy and Stormorken syndrome', *Medecine/Sciences*, 34, pp. 26–31. Available at: https://doi.org/10.1051/medsci/201834s208.

- Calderón, J.C., Bolaños, P. and Caputo, C. (2014a) 'The excitation-contraction coupling mechanism in skeletal muscle', *Biophysical Reviews*, pp. 133–160. Available at: https://doi.org/10.1007/s12551-013-0135-x.

- Calderón, J.C., Bolaños, P. and Caputo, C. (2014b) 'The excitation-contraction coupling mechanism in skeletal muscle', *Biophysical Reviews*, pp. 133–160. Available at: https://doi.org/10.1007/s12551-013-0135-x.

- Chen, W. and Kudryashev, M. (2020a) 'Structure of RyR1 in native membranes', *EMBO reports*, 21(5). Available at: https://doi.org/10.15252/embr.201949891.
- Chen, W. and Kudryashev, M. (2020b) 'Structure of RyR1 in native membranes', *EMBO reports*, 21(5). Available at: https://doi.org/10.15252/embr.201949891.

- Eu, J.P. and Meissner, G. (2012) 'Detection of calcium release via ryanodine receptors', *Methods in Molecular Biology*, 798, pp. 373–382. Available at: https://doi.org/10.1007/978-1-61779-343-1_21.

- Hanna, A.D. *et al.* (2021) 'Pathological mechanisms of vacuolar aggregate myopathy arising from a Casq1 mutation', *FASEB Journal*, 35(5). Available at: https://doi.org/10.1096/fj.202001653RR.

- He, Z. *et al.* (1993) 'Ca^{2+}-induced folding and aggregation of skeletal muscle sarcoplasmic reticulum calsequestrin. The involvement of the trifluoperazine-binding site', *Journal of Biological Chemistry*, 268(33), pp. 24635–24641. Available at: https://doi.org/10.1016/s0021-9258(19)74513-x.

- Heiny, J. and Meissner, G. (2012) 'Excitation-contraction coupling in skeletal muscle', in *Cell Physiology Source Book*. Elsevier Inc., pp. 783–800. Available at: https://doi.org/10.1016/B978-0-12-387738-3.00045-7.

- Kumar, A. *et al.* (2013) 'Identification of calcium binding sites on calsequestrin 1 and their implications for polymerization', *Molecular BioSystems*, 9(7), pp. 1949–

1957. Available at: https://doi.org/10.1039/c3mb25588c.

- Maclennan, D.H. and Wong, P.T.S. (1971) *Isolation of a Calcium-Sequestering Protein from Sarcoplasmic Reticulum (rabbit/deoxycholate/column chromatography/transport)*.

- Manno, C. *et al.* (2017a) 'Calsequestrin depolymerizes when calcium is depleted in the sarcoplasmic reticulum of working muscle', *Proceedings of the National Academy of Sciences of the United States of America*, 114(4), pp. E638–E647. Available at: https://doi.org/10.1073/pnas.1620265114.

- Manno, C. *et al.* (2017b) 'Calsequestrin depolymerizes when calcium is depleted in the sarcoplasmic reticulum of working muscle', *Proceedings of the National Academy of Sciences of the United States of America*, 114(4), pp. E638–E647. Available at: https://doi.org/10.1073/pnas.1620265114.

- Michelucci, A. *et al.* (2019) 'Transverse tubule remodeling enhances Orai1-dependent Ca $^{2+}$ entry in skeletal muscle The functional benefits of exercise on SOCE, constitutive Ca $^{2+}$ entry and muscle force production were lost in mice with muscle-specific loss of Orai1 function. These results indicate that TT association with SR-stacks enhances Orai1-dependent SOCE to optimize Ca $^{2+}$ dynamics and muscle contractile function during acute exercise'. Available at: https://doi.org/10.7554/eLife.47576.001.

- Michelucci, A. *et al.* (2020) 'Pre-assembled Ca^{2+} entry units and constitutively active Ca^{2+} entry in skeletal muscle of calsequestrin-1 knockout mice', *Journal of General Physiology*, 152(10). Available at: https://doi.org/10.1085/JGP.202012617.

- Mukund, K. and Subramaniam, S. (2020a) 'Skeletal muscle: A review of molecular structure and function, in health and disease', *Wiley Interdisciplinary Reviews: Systems Biology and Medicine*. Wiley-Blackwell. Available at:

https://doi.org/10.1002/wsbm.1462.

- Mukund, K. and Subramaniam, S. (2020b) 'Skeletal muscle: A review of molecular structure and function, in health and disease', *Wiley Interdisciplinary Reviews: Systems Biology and Medicine*. Wiley-Blackwell. Available at: https://doi.org/10.1002/wsbm.1462.

- Nelson, H.A. *et al.* (2018) 'Interplay between ER Ca^{2+} binding proteins, STIM1 and STIM2, is required for store-operated Ca^{2+} entry', *International Journal of Molecular Sciences*, 19(5). Available at: https://doi.org/10.3390/ijms19051522.

- Putney, J.W. (2011) 'The physiological function of store-operated calcium entry', *Neurochemical Research*, pp. 1157–1165. Available at: https://doi.org/10.1007/s11064-010-0383-0.

- Roberts, M.D. *et al.* (2020) 'An optimized procedure for isolation of rodent and human skeletal muscle sarcoplasmic and myofibrillar proteins', *Journal of Biological Methods*, 7(1), p. e127. Available at: https://doi.org/10.14440/jbm.2020.307.

- Rossi, D. *et al.* (2008) 'The sarcoplasmic reticulum: An organized patchwork of specialized domains', *Traffic*, pp. 1044–1049. Available at: https://doi.org/10.1111/j.1600-0854.2008.00717.x.

- Rossi, D. *et al.* (2014) 'A Mutation in the CASQ1 Gene Causes a Vacuolar Myopathy with Accumulation of Sarcoplasmic Reticulum Protein Aggregates', *Human Mutation*, 35(10), pp. 1163–1170. Available at: https://doi.org/10.1002/humu.22631.

- Rossi, D. *et al.* (2021a) 'Calsequestrin, a key protein in striated muscle health and disease', *Journal of Muscle Research and Cell Motility*, 42(2), pp. 267–279. Available at: https://doi.org/10.1007/s10974-020-09583-6.

- Rossi, D. *et al.* (2021b) 'Calsequestrin, a key protein in striated muscle health and disease', *Journal of Muscle Research and Cell Motility*, 42(2), pp. 267–279. Available at: https://doi.org/10.1007/s10974-020-09583-6.
- Rossi, D. *et al.* (2022) 'Multiple regions within junctin drive its interaction with calsequestrin-1 and its localization to triads in skeletal muscle', *Journal of Cell Science*, 135(2). Available at: https://doi.org/10.1242/jcs.259185.

- Serafini, M. *et al.* (2019) 'Synthesis, docking and biological evaluation of a novel class of imidazothiazoles as IDO1 inhibitors', *Molecules*, 24(10). Available at: https://doi.org/10.3390/molecules24101874.

- Silva-Rojas, R. *et al.* (2022) 'Silencing of the Ca^{2+} Channel ORAI1 Improves the Multi-Systemic Phenotype of Tubular Aggregate Myopathy (TAM) and Stormorken Syndrome (STRMK) in Mice', *International Journal of Molecular Sciences*, 23(13). Available at: https://doi.org/10.3390/ijms23136968.

- Stafford, N. *et al.* (2017a) 'THE PLASMA MEMBRANE CALCIUM ATPASES AND THEIR ROLE AS MAJOR NEW PLAYERS IN HUMAN DISEASE', *Physiol Rev*, 97, pp. 1089–1125. Available at: https://doi.org/10.1152/phys.

- Stafford, N. *et al.* (2017b) 'THE PLASMA MEMBRANE CALCIUM ATPASES AND THEIR ROLE AS MAJOR NEW PLAYERS IN HUMAN DISEASE', *Physiol Rev*, 97, pp. 1089–1125. Available at: https://doi.org/10.1152/phys.

- Sztretye, M. *et al.* (2017) 'SOCE Is Important for Maintaining Sarcoplasmic Calcium Content and Release in Skeletal Muscle Fibers', *Biophysical Journal*, 113(11), pp. 2496–2507. Available at: https://doi.org/10.1016/j.bpj.2017.09.023.

- Wang, L. *et al.* (2015a) 'Retrograde regulation of STIM1-Orai1 interaction and store-operated Ca^{2+} entry by calsequestrin', *Scientific Reports*, 5. Available at: https://doi.org/10.1038/srep11349.

- Wang, L. *et al.* (2015b) 'Retrograde regulation of STIM1-Orai1 interaction and store-operated Ca^{2+} entry by calsequestrin', *Scientific Reports*, 5. Available at: https://doi.org/10.1038/srep11349.

- Wang, L. *et al.* (2018) 'Thick filament protein network, functions, and disease association', *Comprehensive Physiology*, 8(2), pp. 631–709. Available at: https://doi.org/10.1002/cphy.c170023.

- Wang, Q. and Michalak, M. (2020a) 'Calsequestrin. Structure, function, and evolution', *Cell Calcium*, 90. Available at: https://doi.org/10.1016/j.ceca.2020.102242.

- Wang, Q. and Michalak, M. (2020b) 'Calsequestrin. Structure, function, and evolution', *Cell Calcium*, 90. Available at: https://doi.org/10.1016/j.ceca.2020.102242.

- Woo, J.S. *et al.* (2020) 'Calsequestrin: a well-known but curious protein in skeletal muscle', *Experimental and Molecular Medicine*. Springer Nature, pp. 1908–1925. Available at: https://doi.org/10.1038/s12276-020-00535-1.

- Yarotskyy, V., Protasi, F. and Dirksen, R.T. (2013) 'Accelerated Activation of SOCE Current in Myotubes from Two Mouse Models of Anesthetic- and Heat-Induced Sudden Death', *PLoS ONE*, 8(10). Available at: https://doi.org/10.1371/journal.pone.0077633.

- Zhang, L. *et al.* (2016) 'Calsequestrin-1 Regulates Store-Operated Ca^{2+} Entry by Inhibiting STIM1 Aggregation', *Cellular Physiology and Biochemistry*, 38(6), pp. 2183–2193. Available at: https://doi.org/10.1159/000445574.